

Estimating greenhouse gas emissions at the soil–atmosphere interface in forested watersheds of the US Northeast

Joshua Gomez · Philippe Vidon · Jordan Gross ·
Colin Beier · Jesse Caputo · Myron Mitchell

Received: 7 August 2015 / Accepted: 7 April 2016 / Published online: 17 April 2016
© Springer International Publishing Switzerland 2016

Abstract Although anthropogenic emissions of greenhouse gases (GHG: CO₂, CH₄, N₂O) are unequivocally tied to climate change, natural systems such as forests have the potential to affect GHG concentration in the atmosphere. Our study reports GHG emissions as CO₂, CH₄, N₂O, and CO_{2eq} fluxes across a range of landscape hydrogeomorphic classes (wetlands, riparian areas, lower hillslopes, upper hillslopes) in a forested watershed of the Northeastern USA and assesses the usability of the topographic wetness index (TWI) as a tool to identify distinct landscape geomorphic classes to aid in the development of GHG budgets at the soil atmosphere interface at the watershed scale. Wetlands were hot spots of GHG production (in CO_{2eq}) in the landscape owing to large CH₄ emission. However, on an areal basis, the lower hillslope class had the greatest influence on the net watershed CO_{2eq} efflux, mainly because it encompassed the largest proportion of the study watershed (54 %) and had high CO₂ fluxes relative to other land classes. On an annual basis, summer, fall, winter, and spring accounted for 40, 27, 9, and 24 % of total

CO_{2eq} emissions, respectively. When compared to other approaches (e.g., random or systematic sampling design), the TWI landscape classification method was successful in identifying dominant landscape hydrogeomorphic classes and offered the possibility of systematically accounting for small areas of the watershed (e.g., wetlands) that have a disproportionate effect on total GHG emissions. Overall, results indicate that soil CO_{2eq} efflux in the Archer Creek Watershed may exceed C uptake by live trees under current conditions.

Keywords Greenhouse gas budget · Watershed · CO₂ equivalent · Topographic index

Introduction

Changes in atmospheric greenhouse gas (GHG) concentrations have been linked to large-scale earth system changes such as warming global temperatures, sea level rise, ocean acidification, and changes in snowpack dynamics (IPCC 2013). In 2011, carbon dioxide (CO₂), methane (CH₄), and nitrous oxide (N₂O) concentrations in the atmosphere reached 391 ppm, 1803 ppb, and 324 ppb, respectively, which represent an increase of 40, 150, and 20 % over preindustrial levels (IPCC 2013). Although anthropogenic emissions of GHG are unequivocally tied to these changes, natural systems such as forests have the potential to affect GHG concentration in the atmosphere (Beier et al. 2015). Forest ecosystems store a globally estimated 1146 Pg of carbon, with roughly two thirds of this amount

J. Gomez · P. Vidon (✉) · J. Gross · C. Beier · J. Caputo ·
M. Mitchell
College of Environmental Science and Forestry (SUNY-ESF), The
State University of New York, 1 Forestry Drive, Syracuse, NY
13210, USA
e-mail: pgvidon@esf.edu

Present Address:

J. Gomez
Tectonic Engineering and Surveying Consultants P.C.,
Mountainville, NY 10953, USA

belowground (Dixon et al. 1994). Thus, a thorough characterization of the amount of GHG produced or consumed at the soil–atmosphere interface in forested systems is needed to fully assess the potential of forested environments to regulate GHG concentration in the atmosphere.

Although several studies have documented GHG dynamics at the soil–atmosphere interface in forested environments (Bowden et al. 1993; Castro et al. 1995; Smith et al. 2003; Riveros-Iregui et al. 2007; Ullah and Moore 2011), watershed-scale estimates of GHG emissions are too few to allow for robust estimates of global GHG emission at the soil–atmosphere interface across a variety of forested systems (IPCC 2007; Hashimoto 2012). Furthermore, developing GHG budgets at the watershed scale is complicated by the known spatial and temporal heterogeneity of soil biogeochemical processes such as aerobic respiration (CO₂ source), nitrification and denitrification (N₂O source and sink), methane oxidation (CO₂ source, CH₄ sink), methanogenesis (CO₂ sink, CH₄ source), and the dependence of GHG fluxes on these processes (Hedin et al. 1998; Naiman et al. 2010).

Some studies nevertheless tackle the issue of GHG budget estimates at the watershed scale. For instance, Pacific et al. (2010) and Riveros-Iregui and McGlynn (2009) related GHG fluxes at the watershed scale to landscape position as a strategy to better predict GHG emission across space. In a companion study, Gomez et al. (in review) showed the importance of local landscape geomorphic characteristics in regulating GHG fluxes at the watershed scale. Other studies, such as Hill et al. (2004) and Gold et al. (2001), relate landscape geomorphic characteristics to soil biogeochemical processes (e.g., denitrification), which influence GHG fluxes at the soil–atmosphere interface. Many other studies have also linked landscape geomorphic characteristics (e.g., topography, contributing area, surficial geology) to soil biogeochemical processes, water quality, and soil organic carbon content (Hill 2000; Groffman et al. 2009; Vidon and Hill 2006; Vidon et al. 2010; Jacinthe et al. 2012). Because these variables affect GHG emission (Riveros-Iregui and McGlynn 2009; Pacific et al. 2010; Gomez et al. in review), quantifying GHG emission for a variety of landscape geomorphic classes and developing watershed GHG budgets based on landform classes is a promising avenue for research as a tool to advance the inventory and assessment of natural GHG emissions at the watershed scale.

Within this context, geographic information systems (GIS) are valuable tools to classify watersheds based on landscape hydrogeomorphic classes and subsequently assess a variety of ecosystem processes. In particular, topographic indices, which are often assessed using GIS, are increasingly used to model ecosystem processes such as hydrology, biogeochemical activity, evapotranspiration, erosion, and sedimentation (Quinn et al. 1995). Baker et al. (2001) also utilized GIS models to increase our ability to predict nutrient export via the analysis of the topographic influence on the hydrologic conditions of a study area. Rosenblatt et al. (2001) demonstrated the value of using GIS data to identify various geomorphic settings that were assessed for nitrate removal potential in riparian zones. With respect to topographic indices in particular, their use is especially valuable in classifying the landscape into a variety of geomorphic or hydrogeomorphic classes. For instance, the topographic wetness index (TWI) defined as $TWI = \ln(a/\tan b)$ (where “a” is the accumulated upslope contributing area per unit contour length and “b” is the local slope angle) is often used to assess the general distribution of soil moisture at the watershed scale (Moore et al. 1991) and is widely used in hydrological and biogeochemical studies (Dosskey and Qiu 2010; Walter et al. 2002; Ogawa et al. 2006; Grabs et al. 2012; Ruhoff et al. 2011). Within a given climate zone, a high wetness index indicates an area that has a high propensity to be moist relative to other locations with lower TWI values.

Our objective in this study is to estimate greenhouse gas (GHG) fluxes and characterize their spatial and temporal heterogeneity within a small-forested watershed of the US Northeast. To this end, we measured GHG fluxes (N₂O, CO₂, CH₄) using a sampling design stratified by landscape position, on 22 occasions over a 3-year period, capturing a range of seasonal climatic and flow conditions. To extrapolate GHG point measurements to the watershed scale, we calculated a very high-resolution TWI (based on a <1-m digital elevation model) to derive landscape hydrogeomorphic classes (e.g., wetlands vs. riparian zones vs. hillslopes), and then used the TWI classes to estimate GHG fluxes and their spatiotemporal patterns at the watershed scale. As a GHG budget at the soil–atmosphere interface is developed, we discuss which areas of the landscape contribute the most to GHG fluxes in CO₂-equivalent units (CO_{2eq}), both seasonally and on an annual basis, and discuss the relative importance of soil–atmosphere

GHG efflux relative to global above ground–below ground carbon sequestration by live vegetation.

Materials and methods

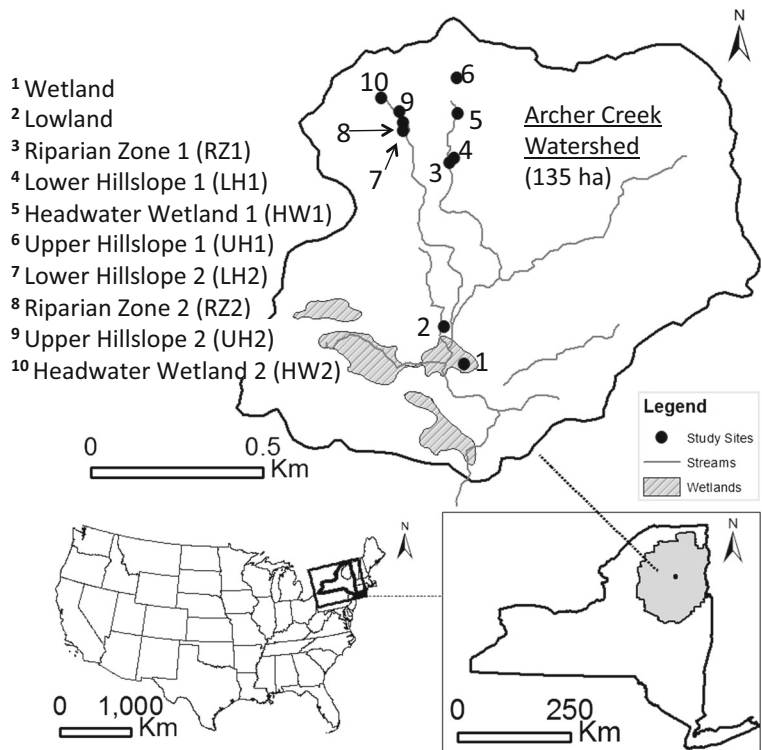
Study area

The Archer Creek Watershed is a 135-ha forested catchment located in the Adirondack region of northern New York State (Fig. 1). Climate is cool, moist, and continental (Shepard et al. 1989). Between the years of 1941–2007, the mean annual temperature in this area was 5.0 °C, the mean annual precipitation was 1046 mm, and the mean annual snowfall was 303 cm (Mitchell et al. 2009). Precipitation in 2011 was 47 % greater than the 30-year average, 8 % less than the 30-year average in 2012, and 12 % greater than the 30-year average in 2013. Snowfall was less than the 30-year average for the entire study period with 3, 52, and 40 % less snowfall occurring in 2011, 2012, and 2013, respectively. Precipitation and air temperature were recorded at the National Deposition Program/National Trends Network Site (ID NY20) located in the Huntington Wildlife Forest approximately 2.0 km from the study area.

Stream discharge for Archer Creek (15 min. interval) was determined for the outlet of Archer Creek watershed where stage height is recorded as part of the ongoing long-term monitoring program of the watershed described in Mitchell et al. (2009).

From a geomorphological standpoint, the Archer Creek catchment has an average slope of 11 %, a total relief of 225 m, and is located within the Anorthosite Massif igneous intrusion, which is composed of up to 90 % calcium-rich plagioclase feldspar (McHale et al. 2002; Mitchell et al. 2009). The surficial geology consists of glacial till, which was deposited by the Wisconsin Glacier approximately 14,000 years ago. The till is composed of approximately 75 % sand, less than 10 % clay content, and includes many boulders and cobblestones (Christopher et al. 2006). The forest soils are classified as Becket–Mundal series sandy loams (coarse-loamy, isotic frigid, Oxyaquic Haplorthods). Upland soils are approximately 1 m thick with localized areas of deeper soil. The O-horizon and Bs-horizon overlay the igneous bedrock and are generally 5 and 80 cm thick, respectively. Wetlands and valley-bottoms located in the Archer Creek Watershed are composed of Greenwood Mucky Peats deposits 1 to 5 m deep (Somers 1986). The lowland overstory in the Archer

Fig. 1 Experimental site location and sampling locations within the Archer Creek Watershed (135 ha). Numbers 1–10 correspond to the sampling locations as indicated on the figure



Creek Watershed is composed of eastern hemlock (*Tsuga Canadensis* (L.) Carr), yellow birch (*Betula alleghaniensis* Britt.), speckled alder (*Alnus incana* (L.) Moench), red spruce (*Picea rubens* Sarg.), and balsam fir (*Abies balsamea* (L.) Mill). American beech (*Fagus grandifolia* Ehrh.), sugar maple (*Acer saccharum* Marsh.), red maple (*Acer rubrum* L.), yellow birch, and eastern white pine (*Pinus strobus* L.) dominate the upland environments (Christopher et al. 2006).

Greenhouse gas sampling and analysis

Ten sampling locations corresponding to the variety of landscape hydrogeomorphic classes found in the watershed (palustrine wetland, lowlands, riparian zones, upper and lower hillslopes, and headwater wetlands; Fig. 1) were selected throughout the Archer Creek Watershed for GHG flux measurements. Although this approach targets specific areas of the watershed for sampling, it is designed to account for all major landscape hydrogeomorphic classes in the watershed that other sampling techniques (e.g., random or stratified sampling design approach) may miss. The lowland was located in a gently sloping area near the palustrine wetland. The riparian zone locations were located immediately adjacent to headwater streams, while the headwater wetlands were located near the source of the two streams used in this study (Fig. 1). The upper hillslope sites were located on generally steep terrain (>20 % slope) while the lower hillslope sites were located downstream of the headwater sites on more moderate slopes (<20 % slope). At each of these sites, greenhouse gas (CO₂, CH₄, N₂O) sampling occurred 19 times during the 2011, 2012, and 2013 snow-free seasons, with an additional 3 winter sampling days in January, February, and March of 2013.

Gas samples for GHG flux calculations at the soil-atmosphere interface were collected using six open top static chambers per site (closed only during sampling), for a total of 60 chambers (Fig. 1). Static chambers were made of white PVC material and consisted of two parts: a bottom section (37 cm height and 27 cm diameter) inserted 5 cm into the ground, and an airtight lid fitted with a gas sampling port installed only during sampling to close the chamber (Jacinthe and Dick 1997). Chambers were only inserted 5 cm into the ground and left untouched during the study period to minimize the impact of chamber installation on shallow root systems. At the time of sampling, soil temperature was recorded

at each sampling location 5 cm below the ground surface using a portable Hanna® pH/ORP/temperature meter (Model HI 9125, Hanna Instrument Inc., Woonsocket, Rhode Island, USA). When sampling, the chambers were closed with the lid and three head-space gas samples were extracted over a period of 50 min. Air samples (~15 mL) were stored in evacuated vials (10 mL) fitted with gray butyl rubber septa. GHG fluxes (F) were computed as follows:

$$F = \left(dC/dt \right) * \left(V/A \right) * k \quad (1)$$

where dC/dt is the rate of change in GHG concentration inside the chamber (mass GHG m³ air per min), V is the chamber volume (m³), A is the area circumscribed by the chamber (m²), and k is a unit conversion factor (1440 min/day) (Jacinthe and Lal 2004). Winter sampling was carried out following the same protocol, except that snow was removed by hand from each chamber immediately before the airtight lid was placed onto the chamber. The snow was returned into the chamber immediately after sampling. Samples were kept out of the light during transport and storage periods and were usually analyzed within 2 weeks of collection.

Carbon dioxide, CH₄, and N₂O concentrations were analyzed utilizing a Shimadzu GC-2014® gas chromatograph (Shimadzu Corporation, Kyoto, Japan) equipped with a flame ionizing detector and an electron capture detector interfaced with a CombiPal® autosampler (LEAP Technologies, Carrboro, North Carolina). The stationary phase consisted of a Porapak Q® precolumn (90 cm long) and Hayesep D® analytical columns (180 cm long). The gas chromatograph (GC) was calibrated using standard gases obtained from Alltech (Deerfield, Illinois). To prevent moisture buildup in the GC columns, the GC oven was heated (150 °C) for 15 min for every 20 samples.

Carbon dioxide, CH₄, and N₂O fluxes at each site were determined by taking the median flux of the six chambers for each sampling date. The CO₂eq flux for CH₄, CO₂, and N₂O fluxes were calculated according to the global warming potential (GWP) values for the 100-year time horizon reported by the International Panel on Climate Change (IPCC 2013). Because CO₂ is the baseline, it has a GWP of 1. The GWP for CH₄ and N₂O are 25 and 298, respectively (IPCC 2013). Seasonal GHG flux calculations were based on astronomical seasons.

We tested for the importance of sampling time on daily soil GHG flux estimates by conducting four intensive sampling campaigns (5-h intervals over a 24-h period) on September 6 and October 20, 2012, and June 6 and July 16, 2013, at one chamber per site (for logistical reasons) at sites RZ1, LH1, RZ2, LH2, HW2, and UH2 (Fig. 1). Carbon dioxide, CH₄, and N₂O fluxes varied over a 24-h period; however, sampling time did not consistently affect flux estimates. Fluxes are therefore reported on a per day basis as opposed to a per hour basis.

Topographic analyses and geomorphic classification of the landscape

A 1-meter resolution bare earth digital elevation model (DEM), derived from discrete LiDAR data collected in 2009, was used to assess the topographic attributes of the Archer Creek Watershed. The topographic wetness index (TWI) was calculated across the watershed using the following equation:

$$TWI = \ln\left(a / \tan b\right) \quad (2)$$

where “a” is the upslope contributing area per unit contour length and “b” is the local slope angle (Beven and Kirkby 1979; Dosskey and Qiu 2010). ArcGIS Model Builder was used to implement the TWI in a stepwise fashion using raster calculator functions. The default algorithm—D8 single flow direction—was used to calculate the flow direction from each cell, and then the flow accumulation for each grid cell was calculated. The D8 single flow direction method apportions all flow from a cell toward the neighboring cell in the steepest downslope direction of one of the eight cardinal directions (Holmgren 1994). A 5 m × 5 m moving average was implemented to smooth, or generalize, the TWI grid, which was then used to classify the watershed into discrete geomorphic classes.

For our study, we used four landscape classes based on TWI thresholds and visual confirmation in the field: wetland, lower hillslope, upper hillslope, and riparian zone. Stream locations were also confirmed by GPS coordinates taken with a Trimble GeoXH GPS unit and each GPS point was accurate to within <0.1 m. The classes based on TWI values ranged from 0 to 1.67, 1.68 to 3.99, 4.00 to 4.70, and 4.71 to 10.70 for the upper hillslope class, the lower hillslope, the riparian zone class, and the wetland

class, respectively. Because the small headwater wetlands had GHG fluxes between those of the riparian zone sites and lower hillslope sites (see the “Results” section) and represented less than 0.5 % of the watershed, they were treated as “riparian zones” or “lower hillslopes” based on their TWI values for landscape geomorphic classification purposes. The lowland site was binned in the lower hillslope category for GHG budget purposes based on TWI values. Finally, when more than one site was found in one category, the arithmetic mean of the each site’s median flux was used for assigning a GHG flux to each geomorphic class.

Uncertainty analysis

In order to better characterize the uncertainty introduced by scaling up plot-level estimates to the entire landscape, we used a resampling (i.e., Monte-Carlo) procedure to estimate the variance around the daily landscape-level GHG flux in CO₂ equivalent. For each combination of season and geomorphic class, we resampled the dataset consisting of the daily median flux values (gCO₂-eq m⁻² day⁻¹) and weighted the resulting mean value by the estimated total acreage under that geomorphic class. We ran this resampling procedure 1000 times, after which we were able to calculate the mean and standard deviation of the resulting sampling distribution ($n=1000$) for each season × geomorphic class combination. Finally, we added together the daily area-weighted flux values of each of the four geomorphic classes to estimate the total daily flux from the entire watershed within each season and took the mean of the four seasons to calculate the average daily flux from the entire watershed throughout the entire year. Analyses were done using the sample function in R version 3.0.2 (R Core Team 2013).

Results

Site hydrology and CO₂, N₂O, and CH₄ fluxes across locations

A detailed description of hydrological conditions and associated CO₂, N₂O and CH₄ emissions are provided in Gomez et al. (in review). Briefly, the 60 static chambers used in this study were sampled across a range of hydrological conditions ranging from high flow to low

flow (measured at the Archer Creek watershed outlet) across all four seasons (3 winter dates, 5 spring dates, 9 summer dates, 5 autumn dates) (Fig. 2). Carbon dioxide fluxes exhibited a strong seasonal pattern (Fig. 3). Regardless of location, winter CO₂ fluxes were significantly smaller and less variable (0.02 to 1.34 g C-CO₂ m⁻² day⁻¹) than during the remainder of the year (-0.77 to 6.87 g C-CO₂ m⁻² day⁻¹). Across locations, the lowland, LH1, UH1, and LH2 sites had mean CO₂ fluxes greater than 2 g C-CO₂ m⁻² day⁻¹ over the study period, while mean CO₂ fluxes at the wetland and RZ1 site were less than 1 g C-CO₂ m⁻² day⁻¹. Other sites (HW1, RZ2, HW2, and UH2) had intermediate CO₂ flux values between 1 and 2 g C-CO₂ m⁻² day⁻¹.

Methane fluxes were highest at the wetland site (range 2 to 1293 mg C m⁻² day⁻¹), with the largest fluxes occurring in the summer and early autumn (July through October). Positive CH₄ fluxes were also observed at the RZ1 site for 18 of the 22 sampling dates; however, CH₄ fluxes were negative on most dates at all other locations.

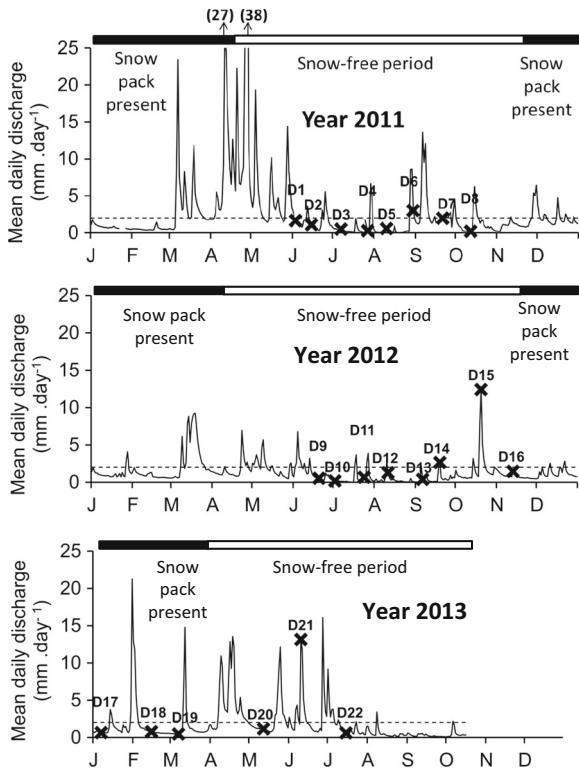


Fig. 2 Daily discharge for years 2011, 2012, and part of 2013 at the Archer Creek Watershed outlet. Labels D1-D22 correspond to the dates when sampling for greenhouse gas emission occurred throughout the watershed. The dashed line indicates the mean annual flow at the watershed outlet

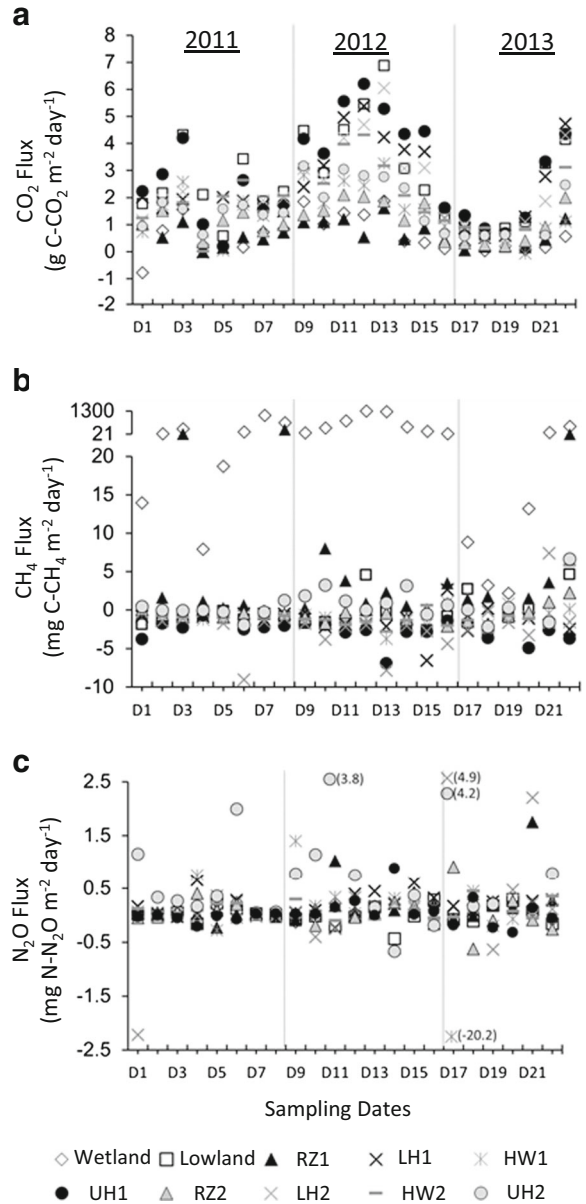


Fig. 3 Median CO₂ (a), CH₄ (b), and N₂O (c) fluxes recorded at each sampling location over the study period. Labels D1-D22 correspond to the sampling dates as described in Fig. 2. Acronyms used in the legend correspond to the sampling locations as described in Fig. 1

When sites were compared, the average study period CH₄ flux at the wetland site (330 mg C m⁻² day⁻¹; Relative Standard Deviation 127 %) was two orders of magnitude higher than the average CH₄ flux at any other site. Nitrous oxide fluxes did not exhibit a strong seasonal pattern or clear differences between locations. On most dates, N₂O fluxes ranged from -0.5 to 0.5 mg N m⁻² day⁻¹.

Average CO₂-equivalent fluxes of GHG across landscape positions

Average CO_{2eq} GHG efflux (sum of g CO_{2eq} for each of CO₂, CH₄, and N₂O) at each site varied among seasons (Table 1). Soil CO_{2eq} GHG emissions at each sampling location were consistently the lowest during the winter season and the highest during summer. Across all locations, the wetland site (palustrine wetland) had the highest CO_{2eq} fluxes in the summer (20.56 g CO_{2eq} m⁻² day⁻¹) and the third lowest CO_{2eq} flux in the winter (0.78 g CO_{2eq} m⁻² day⁻¹). The mean CO_{2eq} GHG efflux for the entire study period (n=22) ranged between 2.98 g CO_{2eq} m⁻² day⁻¹ (RZ1 riparian zone) and 13.27 g CO_{2eq} m⁻² day⁻¹ (wetland site) across the study sites (Fig. 4). Carbon dioxide was the primary contributor to the positive CO_{2eq} fluxes at each of the ten sampling locations except at the wetland site where CH₄ contributed 83 % of average CO_{2eq} fluxes over the study period. The CO₂ flux comprised more than 100 % of the net positive CO_{2eq} GHG flux at the lowland, HW1, and UH1 sites owing to negative CO_{2eq} fluxes of N₂O and/or CH₄ at these sampling locations. During the study period N₂O flux expressed in CO_{2eq} ranged between -0.34 to 0.38 g CO_{2eq} m⁻² day⁻¹ across the landscape. The N₂O flux contributions to the net daily CO_{2eq} fluxes were very small (~1 % CO_{2eq} emissions in most cases) compared to the contributions of CH₄ fluxes in the wetland or CO₂ fluxes at all other locations to total CO_{2eq} emissions (Fig. 4).

Table 1 Mean CO_{2eq} flux for the wetland, lowland, RZ1—riparian zone (RZ1), LH1—lower hillslope (LH1), HW1—headwater wetland (HW1), UH1—upper hillslope

Site	g CO _{2eq} m ⁻² day ⁻¹			
	Winter (n=3)	Spring (n=5)	Summer (n=9)	Autumn (n=5)
Wetland	0.78	3.40	20.56	17.50
Lowland	2.90	9.35	13.98	7.80
RZ1	0.56	2.60	3.37	4.09
LH1	2.43	7.40	11.57	8.81
HW1	-1.23	4.58	6.76	5.15
UH1	3.42	10.03	13.38	10.08
RZ2	0.93	3.78	5.80	3.70
LH2	3.01	6.72	11.39	8.23
HW2	3.07	5.52	9.64	5.94
UH2	2.86	5.00	8.05	5.08

The number (n) of sampling dates is reported for each season

Topographic and geomorphic classification of the Archer Creek Watershed

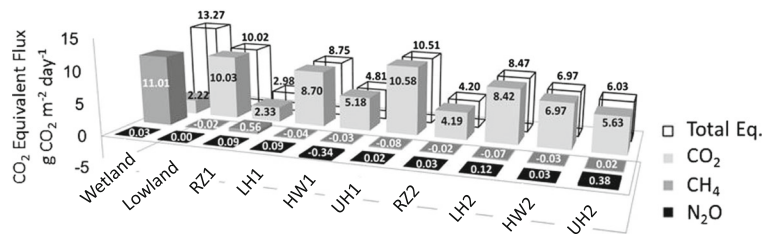
The slope of the land surface in the Archer Creek watershed ranged between 0 and 77° (Fig. 5). The TWI index ranged from 0 (least propensity to be saturated) to 15.88 (greatest propensity to be saturated) with an average of 1.87 (±2.12) (Fig. 5). Following the 5 m × 5 m moving average smoothing procedure described in the “Materials and methods” section, the generalized (smoothed) TWI values across the watershed ranged between 0 and 10.70. The total geomorphic areal contributions were 46.6, 72.5, 6.83, and 7.62 ha for the upper hillslope, lower hillslope, riparian area, and wetland categories, respectively (Fig. 5). These geomorphic areas were adjusted to account for the estimated stream area of 12,075 m² (i.e., stream areas were excluded from geomorphic classes). The lower hillslope class comprised the largest portion of the watershed area (54 %) followed by the upper hillslope (35 %), wetland (5.7 %), riparian area (5 %), and stream (1 %) classes.

Area-weighted CO_{2eq} GHG budgets for the Archer Creek Watershed

Extrapolating average seasonal CO_{2eq} fluxes recorded for each season for each geomorphic class on an areal basis resulted in estimated daily winter, spring, summer, and autumn GHG fluxes at the soil-atmosphere interface of 3.60 × 10⁶, 9.65 × 10⁶, 1.58 × 10⁷, and 1.11 × 10⁷ g

(UH1), RZ2—riparian zone (RZ2), LH2—lower hillslope (LH), HW2—headwater wetland (HW), and UH2—upper hillslope (UH2) sites for each season of the year

Fig. 4 Mean CH₄, CO₂, and N₂O fluxes in CO₂eq for each sampling location (see N for sampling location acronym definition) over the study period



CO₂eq day⁻¹, respectively (Table 2). When the average daily CO₂eq fluxes for each landscape class were combined, the watershed CO₂eq efflux due to CO₂ was at least an order of magnitude greater than the CO₂eq efflux due to CH₄ and N₂O fluxes across the four seasons. The Archer Creek Watershed was a net CH₄ sink (-3.28×10^4 g CO₂eq day⁻¹) during the winter season, but was a net source for all other seasons. When

seasonal averages are considered across all land classes, the annual GHG budget for the entire watershed was 1.01×10^7 g CO₂eq day⁻¹ or 3.68 Gg CO₂eq year⁻¹. The summer, fall, winter, and spring seasons accounted for 40, 27, 9, and 24 % of the annual CO₂eq budget from the Archer Creek Watershed.

Overall, the influence of CO₂ flux across the landscape was the greatest, with CO₂ flux contributing

Fig. 5 Various stages of the landscape classification procedure based on the hydrogeomorphic characteristics of the Archer Creek watershed: **a** hillshade view of the topography of the watershed and sampling site location (white dots), **b** slope, **c** topographic wetness index (TWI); and **d** generalized geomorphic classes of the watershed. Numbers in parenthesis indicate the surface area of each land class

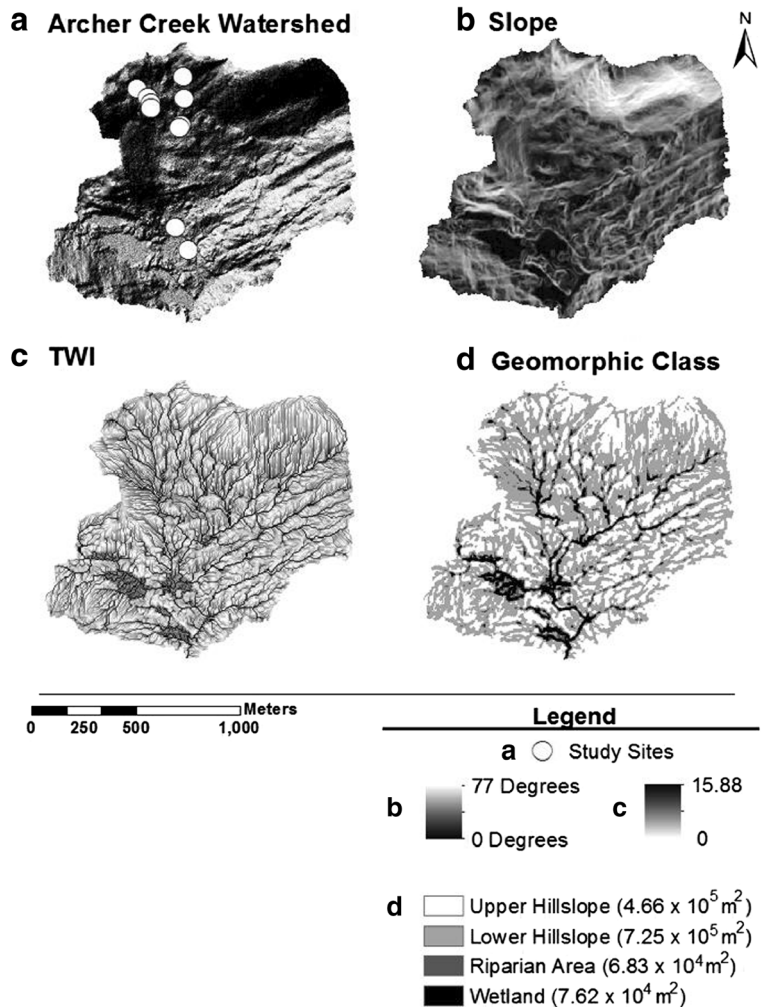


Table 2 Winter, spring, summer, and autumn daily GHG flux for the entire Archer Creek watershed (135 ha) in CO_{2eq} (left column), and daily CH₄, CO₂, and N₂O fluxes in CO_{2eq} for each landscape hydrogeomorphic class and each season (columns 3, 4, 5)

	Geomorphic classification and % total area	CH ₄ (g CO _{2eq} day ⁻¹)	CO ₂ (g CO _{2eq} day ⁻¹)	N ₂ O (g CO _{2eq} day ⁻¹)
Winter	Upper hillslopes (35 %)	-2.07 × 10 ⁴	1.32 × 10 ⁶	1.63 × 10 ⁵
Winter daily watershed budget 3.60 × 10 ⁶ g CO _{2eq} d ⁻¹	Lower hillslopes (54 %)	-2.36 × 10 ⁴	1.85 × 10 ⁶	1.89 × 10 ⁵
	Riparian areas (5 %)	-6.03 × 10 ²	5.00 × 10 ⁴	1.62 × 10 ³
	Wetlands (5.7 %)	1.21 × 10 ⁴	4.36 × 10 ⁴	3.83 × 10 ³
	All areas combined	-3.28 × 10 ⁴	3.27 × 10 ⁶	3.58 × 10 ⁵
	Upper hillslopes (35 %)	-2.13 × 10 ⁴	3.48 × 10 ⁶	4.77 × 10 ⁴
Spring daily watershed budget 9.65 × 10 ⁶ g CO _{2eq} d ⁻¹	Lower hillslopes (54 %)	-1.94 × 10 ⁴	5.66 × 10 ⁶	3.30 × 10 ⁴
	Riparian areas (5 %)	1.34 × 10 ³	2.10 × 10 ⁵	6.59 × 10 ³
	Wetlands (5.7 %)	1.43 × 10 ⁵	1.16 × 10 ⁵	5.59 × 10 ²
	All areas combined	1.03 × 10 ⁵	9.46 × 10 ⁶	8.78 × 10 ⁴
	Upper hillslopes (35 %)	-1.23 × 10 ⁴	4.90 × 10 ⁶	1.07 × 10 ⁵
Summer daily watershed budget 1.58 × 10 ⁷ g CO _{2eq} d ⁻¹	Lower hillslopes (54 %)	-3.49 × 10 ⁴	8.94 × 10 ⁶	2.72 × 10 ⁴
	Riparian areas (5 %)	9.67 × 10 ³	3.00 × 10 ⁵	3.57 × 10 ³
	Wetlands (5.7 %)	1.30 × 10 ⁶	2.61 × 10 ⁵	2.73 × 10 ³
	All areas combined	1.26 × 10 ⁶	1.44 × 10 ⁷	1.41 × 10 ⁵
	Upper hillslopes (35 %)	-1.08 × 10 ⁴	3.53 × 10 ⁶	1.43 × 10 ⁴
Autumn daily watershed budget 1.11 × 10 ⁷ g CO _{2eq} d ⁻¹	Lower hillslopes (54 %)	-3.95 × 10 ⁴	6.01 × 10 ⁶	3.16 × 10 ⁴
	Riparian areas (5 %)	6.37 × 10 ⁴	1.99 × 10 ⁵	3.26 × 10 ³
	Wetlands (5.7 %)	1.20 × 10 ⁶	1.34 × 10 ⁵	3.16 × 10 ³
	All areas combined	1.21 × 10 ⁶	9.88 × 10 ⁶	5.23 × 10 ⁴
	All areas combined	6.35 × 10 ⁵	9.25 × 10 ⁶	1.58 × 10 ⁵

Average Annual Daily Watershed GHG budget: 1.01 × 10⁷ g CO_{2eq} day⁻¹. Annual GHG budget: 3.68 × 10⁹ g CO_{2eq} year⁻¹ or 3.68 Gg CO_{2eq} year⁻¹. The surface area (% total area) of each hydrogeomorphic class is also indicated (column 2)

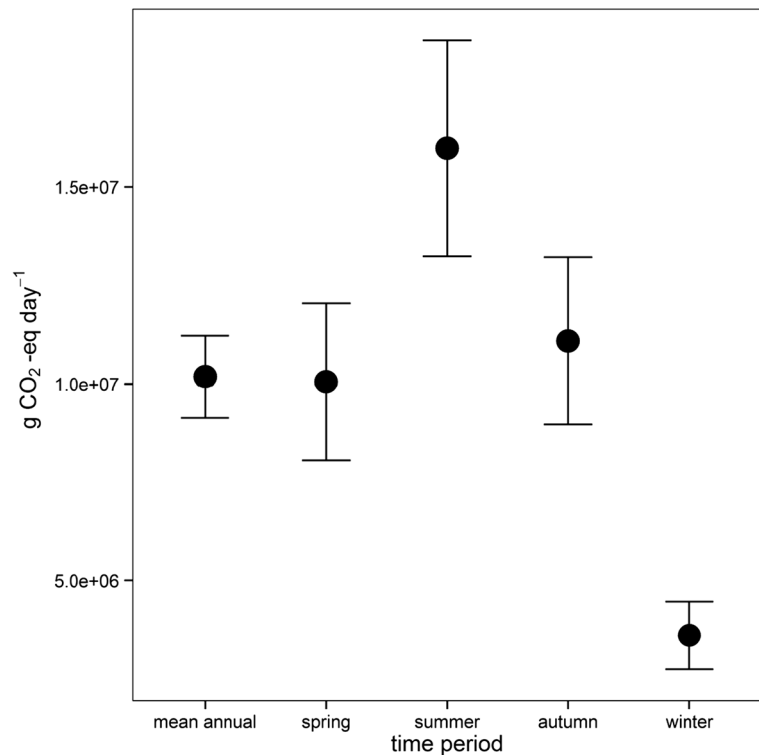
approximately 92 % of the net GHG efflux from the Archer Creek Watershed on a daily basis. Methane emission comprised 6.94 % of the net average daily CO_{2eq} efflux across the watershed, while N₂O fluxes comprised just over 1 % of the annual net CO_{2eq} emissions in the whole watershed. The upper and lower hillslopes (which comprise 90 % of the Archer Creek Watershed Area) were combined CH₄ sinks on the order of -4.56 × 10⁵ g CO_{2eq} day⁻¹, partially offsetting the combined positive CH₄ efflux of 6.80 × 10⁵ g CO_{2eq} day⁻¹ from the riparian and wetland areas.

Uncertainty analysis for area-weighted CO_{2eq} GHG budgets

The mean daily carbon flux from the Archer Creek watershed plus two standard errors (i.e., standard deviations of the sampling distribution) was equal to 1.01 × 10⁷ ± 1.05 × 10⁶ g CO_{2eq} day⁻¹ (Fig. 6); in

other words (according to the central limit theorem), >95 % of our resampled values fell within 10 % of the initial point estimate. Compared to the annual mean, estimated uncertainty was greatest during the summer (2 SE = 2.75 × 10⁶ g CO_{2eq} day⁻¹) and least during the winter season (2 SE = 8.67 × 10⁵ g CO_{2eq} day⁻¹). The uncertainty associated with daily total flux measurements differed across geomorphic class (Fig. 7). The least certain contribution to the annual landscape carbon flux was associated with the lower hillslope region during the summer (2 SE = 2.23 × 10⁶ g CO_{2eq} day⁻¹), which is the largest category (54 % of the watershed area) as well as the category with the greatest variability of methane fluxes as compared to carbon dioxide and nitrous oxide fluxes. In the summer, when methane fluxes are highest, uncertainty estimates around the wetland fluxes (2 SE = 8.59 × 10⁵ g CO_{2eq} day⁻¹) are more than an order of magnitude greater than those around

Fig. 6 Total daily carbon fluxes in CO_{2eq} for Archer Creek watershed on an annual and seasonal basis. Error bars represent two standard errors as calculated as part of the uncertainty analysis using Monte-Carlo analysis ($n = 1000$)



the fluxes from the riparian zones ($2 \text{ SE} = 7.72 \times 10^4 \text{ g CO}_{2\text{eq}} \text{ day}^{-1}$).

Discussion

Impact of landscape position on CO₂, N₂O, CH₄, and total CO₂ equivalent

As discussed in details in Gomez et al. (in review), the GHG fluxes measured in this study were consistent with previously published results (Bowden et al. 1993; Riveros-Iregui and McGlynn 2009; Ullah and Moore 2011; Jacinthe et al. 2012; Morse et al. 2012; Turetsky et al. 2014). Similarly, when converted to CO₂ equivalent, our results are consistent with other studies. For instance, Jungkunst et al. (2008) reported CO₂ equivalent fluxes between 8.9 and 13.2 g CO_{2eq} m⁻² day⁻¹ in a mineral hydromorphic soil in a cool-humid forested watershed dominated by Norway Spruce in Germany. Jungkunst et al. (2008) also reported CO_{2eq} fluxes across a range of induced moisture conditions with ranges of 6.3 to 20.4 g CO_{2eq} m⁻² day⁻¹ and 6.0 to 19.1 g CO_{2eq} m⁻² day⁻¹ in a mineral soil with peat layers and in a purely organic soil,

respectively. When converted to CO₂ equivalent, the CH₄, N₂O, and CO₂ fluxes reported by Ullah and Moore (2011) in forested catchments in Quebec, Canada were 5.1, 4.5, and 4.0 g CO_{2eq} m⁻² day⁻¹ at an Old Growth Upland, Old Growth riparian, and a wetland site, respectively. Although these CO_{2eq} flux magnitudes were generally smaller than those reported in our study (Table 1), the degree of influence of each gas on the net CO_{2eq} flux was similar to those in our study (Fig. 4).

The importance of CH₄ emissions in driving total CO_{2eq} emissions at the wetland site is consistent with the highly reduced conditions often observed in wetlands, which promote methanogenesis and high rates of CH₄ emission (Groffman and Pouyat 2009; Morse et al. 2012). Our findings also suggest that the CO_{2eq} flux of riparian areas, which are areas in the landscape that are often saturated and may promote reduced conditions, were influenced largely by CO₂ fluxes rather than CH₄ (Fig. 4). This suggests that anaerobic conditions did not persist for sufficiently long periods of time at these locations to promote CH₄ production as observed at the wetland site. Generally, the same areas associated with high CO₂ flux are CH₄ sinks, though these sinks account for less than 1 % of the net positive CO_{2eq} flux in this study (Fig. 4).

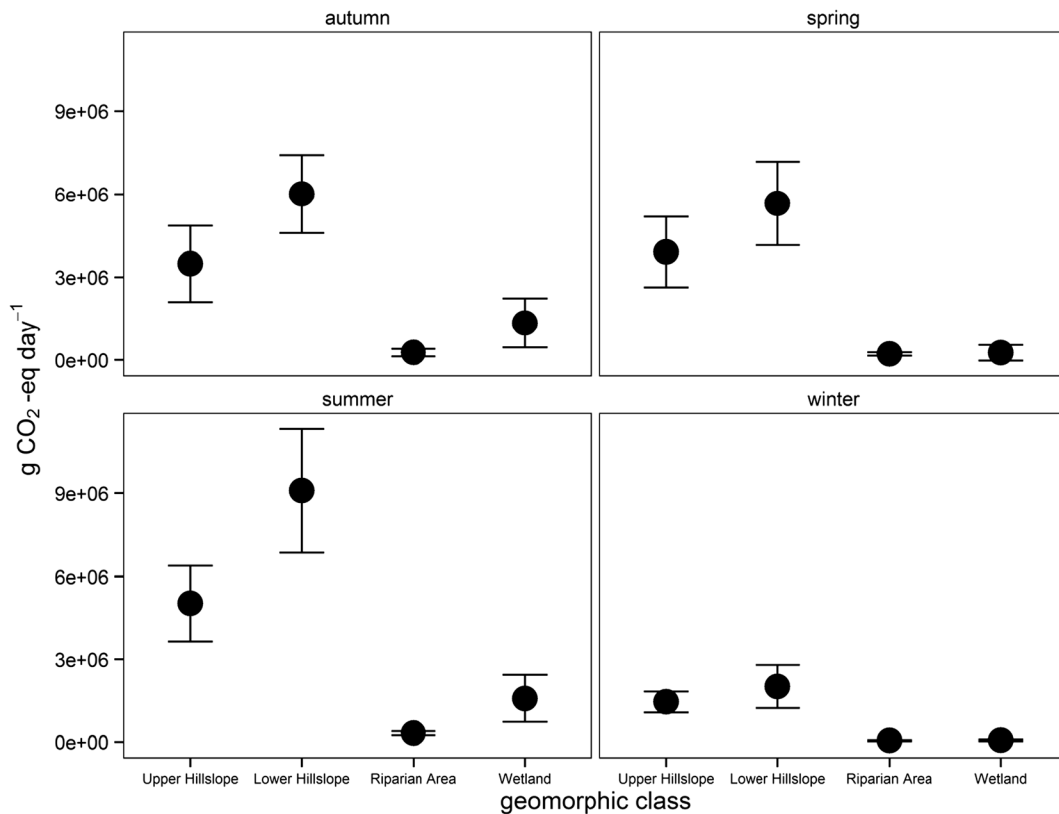


Fig. 7 Total daily carbon fluxes in CO_{2eq} for each geomorphic class in Archer Creek watershed on a seasonal basis. Error bars represent two standard errors as calculated as part of the uncertainty analysis using Monte-Carlo analysis ($n = 1000$)

In terms of seasonality, the highest net CO_{2eq} fluxes at each of the sampling sites throughout the year were recorded during the summer months, which were associated with high CO₂ fluxes across the watershed, and high CH₄ fluxes at the wetland site. These elevated fluxes can be attributed to higher soil temperatures and increased belowground microbial and root respiration (Davidson et al. 1998; Bowden et al. 1998). Autumn and spring net CO_{2eq} GHG fluxes at each site were similar except at the wetland site where autumn CO_{2eq} flux was 17.50 g CO_{2eq} m⁻² day⁻¹ and that of the spring was 3.40 g CO_{2eq} m⁻² day⁻¹. Lower spring CO₂ fluxes at the wetland site were likely due to the wetland remaining frozen late into spring (personal observation) and high water levels induced by spring snow melt, which would limit gas diffusion (Davidson et al. 1998). This variation in GHG fluxes between the winter and summer seasons has implications for the calculation of annual GHG flux estimates. For instance, by sampling for greenhouse gas fluxes only during growing seasons, important fluctuations in greenhouse gas

emissions due to seasonal trends in moisture patterns, temperature patterns, respiration (both autotrophic and heterotrophic), and photosynthesis may be missed (Rosenbaum et al. 2012; Carrara et al. 2004; Monson et al. 2006). If these temporal changes in GHG fluxes are not measured, total CO_{2eq} GHG budgets will not provide accurate estimates of the forest soil contribution to GHG fluxes to the atmosphere on an annual basis. Our data suggests that sampling only during the growing season and extrapolating to the entire year would result in overestimates of GHG fluxes to the atmosphere.

Pros and cons of using the TWI method to identify landscape geomorphic classes and validation of land class estimates

Freer et al. (1997) indicate that knowledge of the hydrologic and biogeochemical functions of the watershed is necessary in order to implement the TWI method. Rodhe and Seibert (1999) also indicate that

TWI results are often validated using stream hydrographs or by validating the predicted saturated overland flow or wetland occurrence in the landscape. Thus, TWI approaches offer a tool to generalize landscape analysis across location, but they should be validated in the field. In this study, we used ground survey measurements and selected GPS points (<1 m accuracy) to ensure that the TWI results accurately represented the moisture patterns in the watershed. In general, the TWI method gave an accurate portrayal of hydrological conditions in the watershed, with highest TWI values (indicating the highest propensity to be saturated) at known stream locations and lowest TWI values (indicating least propensity to be saturated) at known steep hillslope areas.

Although the TWI method is a useful tool to help identify locations in the landscape with a high propensity to be saturated, several assumptions were made when applying the TWI methodology to our watershed: (1) soil hydraulic conductivity and soil depth are uniform across the watershed; (2) topography represents the underlying geologic gradient; (3) local slope angles are representative of the downward hydraulic gradient; and (4) the resolution of the topographic data are high enough to sufficiently capture changes in topographic conditions. In addition to the fact that previous studies have shown that topography can be a useful predictor for soil moisture potential in mountainous regions (Nippgen et al. 2011; Riveros-Iregui and McGlynn 2009), field observations indicated the presence of very shallow soil above glacial till (confining layer for groundwater) in Archer Creek Watershed. It is therefore likely that the Archer Creek Catchment topography reflects the subsurface geologic gradient. Furthermore, our study used high resolution (1 m) topographic data in order to best capture small-scale topographic changes. High resolution Lidar data has been shown to be a good representation of the actual ground surface, especially in comparison to digital elevation models (DEMs) derived from topographic contour maps (Vaze et al. 2010). Therefore, we believe that in our study, the local slope angle is captured at a high resolution and represents an accurate downward hydraulic gradient. Nevertheless, it is important to note that the use of high resolution topographic data (~1 m) tend to overemphasize local variations in topography and the overemphasis can be propagated in the analysis of topographic wetness indexes, skewing realistic flow and moisture patterns (Buchanan et al. 2013). To

address this limitation, a DEM smoothing procedure was used in our study (see the “Materials and methods” section). Smoothing, or generalization, has been shown to reduce the effect of local topographic anomalies and moderate excessive flow convergence propagated by algorithms used in GIS analysis (Buchanan et al. 2013). The resulting smoothed TWI grid therefore represents a more realistic representation of soil moisture patterns than when implementing the TWI directly on high-resolution data.

The TWI values found in this study fell between 0 and 16, which is consistent with ranges reported in a study by Ruhoff et al. (2011) for a variety of landscapes. The estimated area for the wetland (5 % total surface area) using the TWI procedure described herein is consistent with wetland area estimates previously established in Archer Creek (4 %; Bischoff et al. 2001). This value is also consistent with the overall surface area of wetlands (4 %) in the Adirondack Park (Homer et al. 2007). Assuming a 2-m wide buffer along the approximate stream length of 12,075 m in the Archer Creek watershed, riparian areas would include 3.2 % of the Archer Creek Watershed. We found a slightly higher riparian zone area using the TWI method (5 %), which could be due to wider riparian areas in level terrain along certain stretches of the stream channel. Elsewhere, Riveros-Iregui and McGlynn (2009) estimate riparian areas to be 2 % of a 393-ha forested watershed on Montana, USA. In that study, the authors classified the remainder of the watershed as hillslopes.

Consequently, in spite of the assumptions needed to implement a TWI methodology to identify land classes, this approach provides an effective tool to identify major hydrogeomorphic land classes across multiple watersheds. Given comparable results with estimations of land class areas in Archer Creek and the greater Adirondacks Park offered in other studies (see references above), we believe that the TWI landscape classification methodology proposed here is a viable and easily scalable alternative to extensive field surveying or manual analysis of topographic maps to identify dominant landscape geomorphic classes at the watershed scale.

Applications of the TWI method to GHG budget estimation at the watershed scale

From a soil–atmosphere GHG budget estimation perspective, this TWI landscape classification offers the

advantage of accounting for small areas of the watershed (e.g., wetlands) that have a disproportionate effect on total GHG emissions. As an alternative to this approach, a random sampling design or a systematic sampling design approach would have limited capacity to systematically account for fluxes in areas of the landscape that have a small footprint but large GHG fluxes. Another benefit of this TWI method over a traditional random or stratified sampling design is that it decreases the number of sampling locations needed to accurately capture the heterogeneity of the hydrogeomorphic conditions typically found in a forested watershed.

When the GHG budget at the soil–atmosphere interface was calculated using seasonal averages extrapolated to an areal basis, the lower hillslopes were the greatest influence on the net $\text{CO}_{2\text{eq}}$ watershed GHG efflux, largely because these hillslopes encompass the largest proportion of the Archer Creek Watershed and have high $\text{CO}_{2\text{eq}}$ fluxes (Table 2). Wetlands were a greater $\text{CO}_{2\text{eq}}$ GHG source than riparian areas were, even though the Wetland class had a smaller area, because of high CH_4 emissions during the summer and autumn seasons (Table 2). These results are consistent with higher temperatures and increased biological activity in the soil during the summer season (Bowden et al. 1998; Davidson et al. 1998). Low winter GHG fluxes can be explained by reduced soil microbial activity and depressed autotrophic respiration (Atkin et al. 2000). Frozen soils also likely limited the soil–atmosphere fluxes during the winter.

Over the entire study period, the net GHG flux across the whole Archer Creek watershed (135 ha) was 1.01×10^7 or $3.68 \text{ Gg CO}_{2\text{eq}} \text{ year}^{-1}$, 99 % of which comes from CO_2 and CH_4 emissions as N_2O represents ~ 1 % $\text{CO}_{2\text{eq}}$ emissions in most cases (see the “Results” section). Although fluxes of GHG (mainly CO_2 and CH_4 fluxes) to the atmosphere at the soil–atmosphere interface are only one of the components of a full C budget for the watershed, when put in context with the C sink provided by live vegetation, these fluxes provide new insights into the potential role of forests at regulating GHG emission to the atmosphere. According to Birdsey (1992), live trees in the US Northeast accumulate between 1400 and 2000 lbs C $\text{acres}^{-1} \text{ year}^{-1}$, which converts to an approximate $0.21\text{--}0.30 \text{ Gg C year}^{-1}$ sequestration rate for vegetation in the entire Archer Creek watershed. By comparison, we estimated a $1.0 \text{ Gg C year}^{-1}$

flux from the soil to the atmosphere for the entire Archer Creek Watershed. If we assume the mature forest (>80 year old) approximates the Birdsey (1992) average, C emissions from soil exceed annual C sequestration by 3–5 times. However, recent growth rates based on forest inventory data from Archer Creek (Beier, unpublished data) indicate a lower net annual sequestration rate than Birdsey (1992), which suggests an even larger disparity between fluxes. A full ecosystem C budget at the watershed scale, including estimates of soil C storage and dissolved organic carbon losses to streams, should be the focus of a future study; however, our current results suggest that Archer Creek watershed could be a net source of greenhouse gases in the landscape.

Conclusion

This study reports GHG emission as CO_2 , CH_4 , N_2O , and $\text{CO}_{2\text{eq}}$ fluxes across a range of landscape hydrogeomorphic classes (upper hillslope, lower hillslope, wetland, and riparian zone), and demonstrate a methodology using the topographic wetness index (TWI) to classify the landscape in distinct landscape geomorphic classes for the extrapolation of point measurements to the watershed scale, using a small forested catchment in the US Northeast. Results showed clear differences in both the average study period and average seasonal fluxes at upper hillslope, lower hillslope, wetland, and riparian zone geomorphic landscape positions within the 135-ha Archer Creek Watershed. Results also identified the TWI landscape classification method presented in this study as a viable and scalable tool to identify dominant landscape geomorphic classes in forested watersheds of the US Northeast. When used to estimate GHG fluxes across the entire surface area of the watershed, this TWI landscape classification method offers the possibility of systematically accounting for small areas of the watershed (e.g., wetlands) that have a disproportionately large effect on total GHG emissions. When compared to estimates of average C uptake rates by forest trees in the US Northeast, results suggest that soil $\text{CO}_{2\text{eq}}$ efflux at the Archer Creek Watershed exceeds annual carbon sequestration by vegetation. A more comprehensive ecosystem C budget is needed to assess whether the forest watershed is a net source or sink of greenhouse gases.

Acknowledgements This project was supported by a USDA McIntire-Stennis Formula Grant (award no. NYZ-2611-20-001) to P. Vidon, M. Mitchell, and C. Beier. The support of NYSERDA in providing funds for the monitoring at the Arbutus Watershed and Huntington Forest is also greatly appreciated. The authors would also like to thank Pat McHale, Satish Serchan, Cheryl Glor, and the staff of the Adirondack Ecological Center in Newcomb, NY, for help in the field and laboratory.

References

- Atkin, O. K., Edwards, E. J., & Loveys, B. R. (2000). Response of root respiration to changes in temperature and its relevance to global warming. *New Phytologist*, *147*(1), 141–154.
- Baker, M. E., Wiley, M. J., & Seelbach, P. W. (2001). GIS-based hydrologic modeling of riparian areas: implications for stream water quality. *Journal of the American Water Resources Association*, *37*(6), 1615–1628.
- Beier, C. M., Caputo, J. A., & Groffman, P. M. (2015). Measuring ecosystem capacity to provide regulating services: forest removal and recovery at Hubbard Brook (USA). *Ecological Applications*, *25*(7), 2011–2021.
- Beven, K. J., & Kirkby, M. J. (1979). A physically based, variable contributing area model of basin hydrology. *Hydrological Sciences Bulletin*, *24*, 43–69.
- Birdsey, R. A. (1992). *Carbon storage and accumulation in United States forest ecosystems* (General Technical Report WO-59, p. 51). Washington D.C.: U.S. Department of Agriculture, Forest Service, Washington Office.
- Bischoff, J. M., Bukaveckas, P., Mitchell, M. J., & Hurd, T. (2001). N storage and cycling in vegetation of a forested wetland: implications for watershed N processing. *Water, Air, and Soil Pollution*, *128*(1–2), 97–114.
- Bowden, R. D., Castro, M. S., Melillo, J. M., Stuedler, P. A., & Aber, J. D. (1993). Fluxes of greenhouse gases between soils and the atmosphere in a temperate forest following a simulated hurricane blowdown. *Biogeochemistry*, *21*(2), 61–71.
- Bowden, R. D., Newkirk, K. M., & Rullo, G. M. (1998). Carbon dioxide and methane fluxes by a forest soil under laboratory-controlled moisture and temperature conditions. *Soil Biology and Biochemistry*, *30*(12), 1591–1597.
- Buchanan, B., Fleming, M., Schneider, R., Richards, B., Archibald, J., Qiu, Z., & Walter, M. (2013). Evaluating topographic wetness indices across central New York agricultural landscapes. *Hydrology & Earth System Sciences Discussions*, *10*(11).
- Carrara, A., Janssens, I. A., Curiel Yuste, J., & Ceulemans, R. (2004). Seasonal changes in photosynthesis, respiration and NEE of a mixed temperate forest. *Agricultural and Forest Meteorology*, *126*(1), 15–31.
- Castro, M. S., Stuedler, P. A., Melillo, J. M., Aber, J. D., & Bowden, R. D. (1995). Factors controlling atmospheric methane consumption by temperate forest soils. *Global Biogeochemical Cycles*, *9*(1), 1–10.
- Christopher, S. F., Page, B. D., Campbell, J. L., & Mitchell, M. J. (2006). Contrasting stream water NO_3^- and Ca^{2+} in two nearly adjacent catchments: the role of soil Ca and forest vegetation. *Global Change Biology*, *12*(2), 364–381.
- Davidson, E. A., Belk, E., & Boone, R. D. (1998). Soil water content and temperature as independent or confounded factors controlling soil respiration in a temperate mixed hardwood forest. *Global Change Biology*, *4*(2), 217–227.
- Dixon, R. K., Solomon, A., Brown, S., Houghton, R., Trexler, M., & Wisniewski, J. (1994). Carbon pools and flux of global forest ecosystems. *Science*, *263*(5144), 185–190.
- Dosskey, M., & Qiu, Z. (2010). *A comparison of alternative methods for prioritizing buffer placement in agricultural watersheds for water quality improvement*. Denver: Proceedings of the 10th International Conference on Precision Agriculture.
- Freer, J., McDonnell, J., Beven, K. J., Brammer, D., Burns, D., Hooper, R. P., & Kendal, C. (1997). Topographic controls on subsurface storm flow at the hillslope scale for two hydrologically distinct small catchments. *Hydrological Processes*, *11*, 1347–1352.
- Gold, A. J., Groffman, P. M., Addy, K., Kellog, D. Q., Stolt, M., & Rosenblatt, A. E. (2001). Landscape attributes as controls on ground water nitrate removal capacity of riparian zones. *Journal of the American Water Resources Association*, *37*(6), 1457–1464.
- Gomez, J., Vidon, P., Beier, C., Mitchell, M., & Gross, J. (2016). Spatial and temporal patterns of CO_2 , CH_4 , and N_2O fluxes at the soil-atmosphere interface in a northern forested watershed. *Atmospheric Environment* (In press).
- Grabs, T., Bishop, K., Laudon, H., Lyon, S. W., & Seibert, J. (2012). Riparian zone hydrology and soil water total organic carbon (TOC): implications for spatial variability and upscaling of lateral riparian TOC exports. *Biogeosciences*, *9*(10), 3901–3916.
- Groffman, P. M., & Pouyat, R. V. (2009). Methane uptake in urban forests and lawns. *Environmental Science and Technology*, *43*(14), 5229–5235.
- Groffman, P., Butterbach-Bahl, K., Fulweiler, W., Gold, A., Morse, J., Stander, E., Tague, C., Tonitto, C., & Vidon, P. (2009). Incorporating spatially and temporally explicit phenomena (hotspots and hot moments) in denitrification models. *Biogeochemistry*. doi:10.1007/s10533-008-9277-5.
- Hashimoto, S. (2012). A new estimation of global soil greenhouse gas fluxes using a simple data-oriented model. *PLoS one*, *7*(8), e41962.
- Hedin, L. O., von Fischer, J. C., Ostrom, N. E., Kennedy, B. P., Brown, M. G., & Robertson, G. P. (1998). Thermodynamic constraints on nitrogen transformations and other biogeochemical processes at soil-stream interfaces. *Ecology*, *79*(2), 684–703.
- Hill, A. R. (2000). Stream chemistry and riparian zones. In J. Jones & P. Mulholland (Eds.), *Streams and ground waters* (pp. 83–110). Maryland Heights: Academic.
- Hill, A. R., Vidon, P., & Langat, J. (2004). Denitrification potential in relation to lithology in five headwater riparian zones. *Journal of Environmental Quality*, *33*, 911–919.
- Holmgren, P. (1994). Multiple flow direction algorithms for runoff modeling in grid based elevation models: an empirical evaluation. *Hydrological Processes*, *8*, 327–334.
- Homer, C., Dewitz, J., Fry, J., Coan, M., Hossain, N., Larson, C., Herold, N., McKerrow, A., VanDriel, J. N., & Wickham, J. (2007). Completion of the 2001 National Land Cover

- Database for the Conterminous United States. *Photogrammetric Engineering and Remote Sensing*, 73(4), 337–341.
- IPCC. (2007). In S. Solomon, D. Qin, M. Manning, Z. Chen, M. Marquis, K. B. Averyt, M. Tignor, & H. L. Miller (Eds.), *Climate change 2007: The physical science basis. Contribution of Working Group I to the Fourth Assessment Report of the Intergovernmental Panel on Climate Change* (p. 996). Cambridge and New York: Cambridge University Press.
- IPCC. (2013). Summary for policymakers. In T. F. Stocker, D. Qin, G. K. Plattner, M. Tignor, S. K. Allen, J. Boschung, A. Nauels, Y. Xia, V. Bex, & P. M. Midgley (Eds.), *Climate change 2013: The physical science basis. Contribution of Working Group I to the Fifth Assessment Report of the Intergovernmental Panel on Climate Change*. Cambridge and New York: Cambridge University Press.
- Jacinthe, P. A., & Dick, W. A. (1997). Soil management and nitrous oxide emissions from cultivated fields in southern Ohio. *Soil & Tillage Research*, 41(3–4), 221–235.
- Jacinthe, P. A., & Lal, R. (2004). Effects of soil cover and land-use on the relations flux-concentration of trace gases. *Soil Science*, 169(4), 243–259.
- Jacinthe, P. A., Bills, J. S., Tedesco, L. P., & Barr, R. C. (2012). Nitrous oxide emission from riparian buffers in relation to vegetation and flood frequency. *Journal of Environmental Quality*. doi:10.2134/jeq2011.0308.
- Jungkunst, H. F., Flessa, H., Scherber, C., & Fiedler, S. (2008). Groundwater level controls CO₂, N₂O and CH₄ fluxes of three different hydromorphic soil types of a temperate forest ecosystem. *Soil Biology and Biochemistry*, 40(8), 2047–2054.
- McHale, M. R., McDonnell, J. J., Mitchell, M. J., & Cirimo, C. P. (2002). A field-based study of soil water and groundwater nitrate release in an Adirondack forested watershed. *Water Resources Research*, 38(4), 2-1–2-16.
- Mitchell, M. J., Raynal, D. J., & Driscoll, C. T. (2009). *Response of Adirondack ecosystems to atmospheric pollutants and climate change at the Huntington Forest and Arbutus Watershed: research findings and implications for public policy* (Synthesis Report). Albany: New York State Energy Research and Development Authority (NYSERDA).
- Monson, R. K., Lipson, D. L., Burns, S. P., Turnipseed, A. A., Delany, A. C., Williams, M. W., & Schmidt, S. K. (2006). Winter forest soil respiration controlled by climate and microbial community composition. *Nature*, 439(7077), 711–714.
- Moore, I. D., Grayson, R. B., & Ladson, A. R. (1991). Digital terrain modeling: a review of hydrological, geomorphological, and biological applications. *Hydrological Processes*, 5, 3–30.
- Morse, J. L., Ardón, M., & Bernhardt, E. S. (2012). Greenhouse gas fluxes in southeastern US coastal plain wetlands under contrasting land uses. *Ecological Applications*, 22(1), 264–280.
- Naiman, R. J., Decamps, H., & McClain, M. E. (2010). *Riparia: ecology, conservation, and management of streamside communities*. Burlington: Academic.
- Nippen, F., McGlynn, B. L., Marshall, L. A., & Emanuel, R. E. (2011). Landscape structure and climate influences on hydrologic response. *Water Resources Research*. doi:10.1029/2011WR011161.
- Ogawa, A., Shibata, H., Suzuki, K., Mitchell, M. J., & Ikegami, Y. (2006). Relationship of topography to surface water chemistry with particular focus on nitrogen and organic carbon solutes within a forested watershed in Hokkaido, Japan. *Hydrological Processes*, 20(2), 251–265.
- Pacific, V. J., McGlynn, B. L., Riveros-Iregui, D. A., Welsch, D. L., & Epstein, H. E. (2010). Landscape structure, groundwater dynamics, and soil water content influence soil respiration across riparian–hillslope transitions in the Tenderfoot Creek Experimental Forest, Montana. *Hydrological Processes*, 25(5), 811–827.
- Quinn, P. F., Beven, K. J., & Lamb, R. (1995). The ln(a/tanB) index: how to calculate it and how to use it within the TOPMODEL framework. *Hydrological Processes*, 9, 161–182.
- R Core Team. (2013). *R: A language and environment for statistical computing*. Vienna: R Foundation for Statistical Computing. <http://www.R-project.org/>.
- Riveros-Iregui, D. A., & McGlynn, B. L. (2009). Landscape structure control on soil CO₂ efflux variability in complex terrain: scaling from point observations to watershed scale fluxes. *Journal of Geophysical Research: Biogeosciences*, 114(G2), G02010.
- Riveros-Iregui, D. A., Emanuel, R. E., Muth, D. J., McGlynn, B. L., Epstein, H. E., Welsch, D. L., Pacific, V. J., & Wraith, J. M. (2007). Diurnal hysteresis between soil CO₂ and soil temperature is controlled by soil water content. *Geophysical Research Letters*, 34(17).
- Rodhe, A., & Seibert, J. (1999). Wetland occurrence in relation to topography: a test of topographic indices as moisture indicators. *Agriculture and Forest Meteorology*, 98–99, 325–340.
- Rosenbaum, U., Bogena, H., Herbst, M., Huisman, J., Peterson, T., Weuthen, A., Western, A., & Vereecken, H. (2012). Seasonal and event dynamics of spatial soil moisture patterns at the small catchment scale. *Water Resources Research*, 48(10).
- Rosenblatt, A., Gold, A., Stolt, M., Groffman, P., & Kellogg, D. (2001). Identifying riparian sinks for watershed nitrate using soil surveys. *Journal of Environmental Quality*, 30(5), 1596–1604.
- Ruhoff, A. L., Castro, N. M. R., & Risso, A. (2011). Numerical modelling of the topographic wetness index: an analysis at different scales. *International Journal of Geosciences*, 2(4).
- Shepard, J., Mitchell, M., Scott, T., Zhang, Y., & Raynal, D. (1989). Measurements of wet and dry deposition in a northern hardwood forest. *Water, Air, and Soil Pollution*, 48(1–2), 225–238.
- Smith, K., Ball, T., Conen, F., Dobbie, K., Massheder, J., & Rey, A. (2003). Exchange of greenhouse gases between soil and atmosphere: interactions of soil physical factors and biological processes. *European Journal of Soil Science*, 54(4), 779–791.
- Somers, R. C. (1986). *Soil classification, genesis, morphology and variability of soils found within the central Adirondack region of New York, State University of New York*. Syracuse: College of Environmental Science and Forestry.
- Turetsky, M. R., Kotowska, A., Bubier, J., Dise, N. B., Crill, P., Homibrook, E. R. C., Minkinen, K., Moore, T. R., Myers-Smith, I. H., Nykänen, H., Olefeldt, D., Rinne, J., Saarnio, S., Shurpali, N., Tuittila, E. S., Waddington, J. M., White, J. R.,

- Wickland, K. P., & Wilmking, M. (2014). A synthesis of methane emissions from 71 northern, temperate, and subtropical wetlands. *Global Change Biology*. doi:10.1111/gcb.12580.
- Ullah, S., & Moore, T. R. (2011). Biogeochemical controls on methane, nitrous oxide, and carbon dioxide fluxes from deciduous forest soils in eastern Canada. *Journal of Geophysical Research*, 116, G03010. doi:10.1029/2010JG001525.
- Vaze, J., Teng, J., & Spencer, G. (2010). Impact of DEM accuracy and resolution on topographic indices. *Environmental Modelling and Software*, 25(10), 1086–1098.
- Vidon, P., & Hill, A. R. (2006). A landscape based approach to estimate riparian hydrological and nitrate removal functions. *Journal of the American Water Resources Association*, 42(4), 1099–1112.
- Vidon, P., Allan, C., Burns, D., Duval, T. P., Gurwick, N., Inamdar, S., Lowrance, R., Okay, J., Scott, D., & Sebestyen, S. (2010). Hot spots and hot moments in riparian zones: potential for improved water quality management. *Journal of the American Water Resources Association*, 46(2), 278–298.
- Walter, M. T., Steenhuis, T. S., Mehta, V. K., Thongs, D., Zion, M., & Schneiderman, E. (2002). Refined conceptualization of TOPMODEL for shallow subsurface flows. *Hydrological Processes*, 16(10), 2041–2046.